PHYSICAL REVIEW A VOLUME 49, NUMBER 1 JANUARY 1994

Electron detachment in low-energy collisions of halogen anions with atomic hydrogen

M. A. Huels,* J. A. Fedchak, R. L. Champion, and L. D. Doverspike
Department of Physics, College of William and Mary, Williamsburg, Virginia 23185

J. P. Gauyacq and D. Teillet-Billy
Laboratoire des Collisions Atomiques et Moléculaires, Bâtiment 351, Université de Paris–Sud (Paris XI), 91405 Orsay Cédex, France

(Received 21 June 1993)

Total electron-detachment cross sections σ_e for collisions of F^-, Cl^-, Br^-, and I^- with atomic hydrogen have been measured for relative collision energies E ranging from 0.1 to 20 eV. For F^-, Cl^-, and Br^-, σ_e is found to decrease with increasing E and is fairly well described by a simple orbiting model in which an effective polarizability is used to describe the interaction of the anion with atomic hydrogen at small internuclear separations. For the system I^-+H, σ_e increases with increasing collision energy. The measured σ_e for Cl^-+H is also found to agree well with calculations based on an effective-range approximation. Charge-transfer cross sections have been measured for F^-, Cl^-, and I^-+H and are found to be small.

PACS number(s): 34.50.−s, 34.20.−b, 34.70.+e

I. INTRODUCTION

Among the naturally abundant elements which form stable negative ions, the halogens are characterized by their unusually high electron affinities (EA's), which range from 3.61 eV for chlorine to 3.06 eV for iodine [1]. Although the collisional mechanisms which govern the destruction of halogen anions have received considerable attention in the past, only a few experimental studies have involved atomic hydrogen targets, mainly due to the difficulties of obtaining well-characterized beams of atomic hydrogen at room temperature. The purpose of this paper is to report cross sections for electron-loss mechanisms in collisions of halogen anions with atomic hydrogen. The experiments are performed on a crossed-beam apparatus previously utilized in this laboratory [2,3] to measure charge transfer and electron-detachment cross sections in low-energy collisions of H^-, D^-, O^-, and S^- and H. In the present experiment, electron-loss mechanisms in collisions of halogen anions with atomic hydrogen are investigated for laboratory collision energies ranging from a few eV to 500 eV.

In low-energy collisions of halogen negative ions X^- with atomic hydrogen the anion may be neutralized via

$$X^-+H\rightarrow XH+e^- \quad [\text{associative detachment (AD)}] , \qquad (1)$$

$$X^-+H\rightarrow X+H+e^- \quad [\text{collisional (direct) detachment (CD)}] , \qquad (2)$$

$$X^-+H\rightarrow X+H^- \quad [\text{charge transfer (CT)}] . \qquad (3)$$

For the halogen anions only a very small charge-transfer cross section is expected at low collision energies and processes (1) and (2) are expected to dominate for $E_{\text{lab}}<500$ eV when $X^-=F^-$, Cl^-, Br^-, and I^-.

Reaction (1) and its inverse, dissociative attachment (DA), are found to be of importance in the chemistry of flames [4–6] and play important roles in many gas lasers: in XeCl eximer lasers, for example, HCl is used as the halogen donor, and the destruction of Cl^- via associative detachment with H is of crucial importance to the laser stability [7–9]. Additionally, the anthropogenic introduction of halogen-containing compounds into the atmosphere has lead to considerable interest in the destruction mechanisms of halogen anions in the *D* region of the ionosphere [10–13].

Of all the halogen-anion hydride systems, F^-+H and Cl^-+H have received the most attention from a theoretical point of view, due in part to the number of experimental measurements which exist for these systems. The rate constant for AD in F^-+H has been reported previously [14] to be about 1.6×10^{-9} cm^3/sec at 300 K, which agrees well with the more recent measurement of Smith and Adams [15], who found values of 1.5×10^{-9} and 8×10^{-10} cm^3/sec at 300 and 515 K, respectively. For Cl^-+H the AD reaction rate has been measured at thermal energies by a number of authors [14,16]. In general, good agreement exists between the measurements and the calculations of Gauyacq [17,18] and Haywood and Delos [19], all yielding a value of about 9.5×10^{-10} cm^3/sec. The calculation of Gauyacq, which is based on a zero-range-potential (ZRP) approximation, has also been used to determine the product vibrational distributions for AD in F^- and Cl^-+H at room temperature, and excellent agreement is found with the measurements of Zwier *et al.* [20,21]. The large measured reaction rates for AD indicate that the intermediate anion states formed in the collisions are attractive into the autodetaching region; this has been verified in the case of HF^- by several *ab initio* calculations [22–25] and also for

---

*Present Address: Départment de Médecine Nucléaire et de Radiobiologie, Faculté de Médecine, Université de Sherbrooke, Sherbrooke, Québec, Canada J1H 5N4.

HCl^- by the calculations of Morgan, Burke, and Gillian [26] and by Gorczyca and Norcross [25]. The quasimolecular intermediate ion states of HCl^- and HF^- have been investigated through various electron-scattering experiments, such as those of Rohr and Linder [27], in which vibrational excitation was measured for $e^- + HCl$ and HF. In both cases the integral cross sections for vibrational excitation exhibited sharp peaks at the energetic threshold and additional broad maxima were observed at collision energies of about 2–3 eV. These original experiments of Rohr and Linder showed the scattering to be isotropic in angle, indicating pure *s*-wave scattering. Experimental studies of dissociative attachment have also shown that the total cross section for this process varies stepwise as the electron energy is varied [28] and that the cross section increases substantially with the vibrational excitation of the target [29]. These observations prompted a series of theoretical studies of electron scattering by hydrogen halides and it was recognized rather early that neither the threshold peaks observed for vibrational excitation nor the above features observed for dissociative attachment could be explained by a collision model which

TABLE I. Survey of calculated potential curves for halogen hydride anions. R_c is taken from the corresponding reference. α' is inferred from R_c and $V(R_c)$, where $V(R_c)$ is the Morse potential of Ref. [51] (see Sec. IV A). SEP denotes the static exchange plus polarization model; RASSCF denotes the restricted-active-space self-consistent-field model; PSS denotes the perturbed-stationary-states model; SOCI denotes the second-order configuration-interaction model; RCI and MC-CI are the relativistic and multiconfiguration models; and FOCI is the frozen-orbit CI model.

Reference	Anion	R_c (Å)	α' (Å^3)	Comments
Gorczyca and Norcross [25]	HCl^-	1.48	0.36	SEP results, close-coupling (CC) approximation
	HCl^-	1.7		SE results, CC approximation; $V(1.7$ Å$)$ lies above $Cl^- + H$, $R = \infty^a$
	HF^-	1.01	0.15	SEP results, CC approximation
	HF^-	1.05	0.39	SE results, CC approximation
Åstrand and Karlström [59]	HCl^-	1.6	0.03	RASSCF calculation
Morgan, Burke, and Gillian [26]	HCl^-	1.51	0.3	SEP model, *R*-matrix method
	HCl^-	1.47	0.38	PSS model, *R*-matrix method
Morgan and Burke [24]	HF^-	1.09	0.41	*R*-matrix method
Chapman, Balasubramanian, and Lin [39]	HBr^-	1.72		SOCI calculation; $V(1.72$ Å$)$ lies above $Br^- + H$, $R = \infty^a$
	HBr^-	1.69		RCI calculation; $V(1.69$ Å$)$ lies above $Br^- + H$, $R = \infty^a$
	HI^-	1.85		SOCI calculation
	HI^-	1.88		RCI calculation
O'Neil, Rosmus, and Norcross [52]	HCl^-	1.6	0.03	MC-CI calculation; the crossing point is an extrapolation of the calculation
Bettendorff, Beunker, and Peyerimhoff [23]	HCl^-	1.69		Multireference CI calculation; $V(1.69$ Å$)$ lies above $Cl^- + H$, $R = \infty^a$
	HF^-	1.38	0.1	Multireference CI calculation
Gauyacq [18]	HCl^-	1.38	0.43	The HCl^- curve of Ref. [18] is not an *ab initio* calculation, but a fit to experimental data
Krauss and Stevens [60]	HCl^-	1.67		FOCI calculation. $V(1.67$ Å$)$ lies above $Cl^- + H$, $R = \infty^a$
Segal and Wolf [22]	HF^-	1.06	0.4^b	CI and stabilization method
Goldstein, Segal and Wetmore [54]	HCl^-	1.57	0.14^b	CI and stabilization method

[a] $V(R)$ is the Morse potential taken from Ref. [51].

[b] This value of α' is used in the classical model described in Sec. IV A.

utilizes a local resonance theory [30,31]. However, all of these observations were accounted for in either nonresonant [31–33] or nonlocal resonant theories [34,35]. More recently, electron-scattering experiments by Knoth *et al.* [36] with HF and HCl targets have been performed with higher resolution than those of Rohr and Linder. They also find sharp peaks at the energetic thresholds for vibrational excitation and, in the case of HCl but *not* HF, a broad maximum is seen for collision energies in the range of 2–3 eV. Unlike Rohr and Linder, however, Knoth and co-workers find the angular dependence of electron scattering to be nonisotropic and suggest that the scattering process requires the consideration of higher partial waves (i.e., *s*, *p*, and *d*). These considerations, are taken into account in recent *ab initio* HCl^- and HF^- potential curve calculations [24–26]. These calculations all agree on the general shape of the ground-state intermolecular potentials for the molecular anion HX^-: it is attractive and crosses or merges with the intermolecular potential for HX in the vincinity of the HX equilibrium position. Table I contains a survey of calculations for these molecular anions which have appeared during the past 15 years. The interested reader can find further theoretical considerations of electron scattering in the review article by Morrison [37].

In contrast to F^- and Cl^-, few theoretical studies have concentrated on the collisional systems formed by I^- or $Br^- + H$, and experimental work has focused on thermal energy measurements. Smith and Adams [15] have measured the rate constant for AD in $Br^- + H$ at 300 and 515 K and found a constant value of 7×10^{-10} cm^3/sec. For AD in $I^- + H$, they found a reaction rate of 3×10^{-10} cm^3/sec at 300 K and 6×10^{-10} cm^3/sec at 515 K; the former value is about five times greater than the upper limit for this reaction as determined by Fehsenfeld [14]. Cross sections for DA in collisions of electrons with HI have been measured by Alajajian and Chutjian [38]; they report approximate potential curves for HI^- which are based upon their measurements. Chapman, Balasubramanian, and Lin [39] have calculated potential curves for several electronic states of HBr^- and HI^-, but no calculations exist for electron-detachment cross sections.

In this paper, we report measurements and a semiclassical effective range calculation of the total electron-detachment cross section for collisions of $Cl^- + H$ and measurements for F^-, Br^-, and $I^- + H$, for laboratory collision energies ranging from about 5 to 500 eV. All of these experimental results are also described in terms of a simple orbiting model [40] in which an adjustable polarizability is used to mimic the salient feature of the anion potential, viz. the point at which the anion potential merges with that of the neutral parent molecule.

II. EXPERIMENTAL APPARATUS AND PROCEDURE

The apparatus used for the total cross-section measurements reported here is of the crossed-beam configuration and has been described in detail elsewhere [2,3]. Only a brief outline of the experimental technique shall be given below.

The negative halide ions F^-, Cl^-, Br^-, and I^- are produced in a discharge source, and the source gas consists of mixture of Ar and CF_4 (6%), Ar and CCl_4 (2%), Ar and CH_3Br (6%), or Ar and CH_3I (2%), respectively. For the production of Cl^- one may also use a mixture of Ar and CH_3Cl (20%).

The negative-ion beam is extracted, mass selected, and subsequently focused by a series of Einzel lenses into the collision region which consists of a 30° section of a cylindrical electrostatic energy analyzer. The small transverse electric field maintained across the analyzer section allows the ion beam to pass through resonantly; the primary beam intensity is monitored by a Faraday cup and the laboratory energy distribution may be determined by a series of grids before and after the primary ion beam passes through the collision region. The maximum halogen anion beam intensities delivered to the collision region range from 2 to 5 nA, with an energy spread of approximately 0.6 eV for the lowest laboratory collision energy and 15 eV for the highest. The resolution of the mass analyzer is sufficient to clearly resolve the natural isotopes of Cl and Br.

Halfway through the cylindrical analyzer section the ion and neutral target beams intersect at right angles; slow product ions and electrons are extracted orthogonally to the plane defined by the reactants. The products pass through a region of magnetic field which separates electrons from product ions which are a result of charge transfer. These scattered products are detected by conventional particle multipliers and their outputs are amplified *in vacuo*.

The atomic hydrogen beam is produced in a commercially available rf discharge source [41] operating at 36 MHz. The dissociation fraction is about 40% and its determination has been described in detail elsewhere [2,3]. From the system of $F^- + H$, the dissociation fraction may be determined by an alternative method. The system $F^- + H_2$ exhibits a peak in the ion production cross section [42] at a relative collision energy of about 2.1 eV which corresponds to a laboratory energy E_L of 22 eV. An estimate of the dissociation fraction may be obtained by directly observing the diminution of this peak when the rf power is turned on, since, for $E_L \leq 52$ eV, charge transfer cannot occur for collisions of $F^- + H$. The dissociation fraction so defined agrees with that obtained via the method of Ref. [3] to within about 5%. The atomic hydrogen source is joined to the vacuum system by means of a precision three-dimensional manipulator, allowing a separate gas nozzle to be moved into place such that alternate target gases may be admitted into the scattering region.

The total electron-detachment cross sections $\sigma_e(E)$ for collisions of F^-, Br^-, and $I^- + H$ are obtained by direct normalization to a calculation for the system $Cl^- + H$, which is presented in Sec. III. If, after background subtraction and correction for the dissociation fraction [2], the product electron signals for $Cl^- + H$ and $X^- + H$ obtained with identical target conditions are defined by $\mathcal{I}_{Cl}(E_L)$ and $\mathcal{I}_X(E_L)$, respectively, then the total absolute electron detachment cross sections for $X^- + H$ is given by

$$\sigma_X(E_L)=\frac{\mathcal{J}_X(E_L)}{\mathcal{J}_{\mathrm{Cl}}(E_L)}\sigma_{\mathrm{Cl}}(E_L)\ , \tag{4}$$

where $\sigma_{\mathrm{Cl}}(E_L)$ is a fit to the calculated total electron-detachment cross section for $\mathrm{Cl}^-+\mathrm{H}$. Thus electron-detachment cross sections may be determined without absolute knowledge of the transmission function for the product electron-detection system [2].

To independently measure $\sigma_e(E)$ for $\mathrm{Cl}^-+\mathrm{H}$ and ascertain the validity of the normalization procedure described above, a procedure identical to that of Ref. [2] is used: the transmission function for the electron-detection system is determined by measuring the known electron-detachment cross sections for $\mathrm{Cl}^-+\mathrm{O}_2$ [43] and $\mathrm{H}^-+\mathrm{O}_2$ [44]. The absolute total cross sections for electron production in $\mathrm{Cl}^-+\mathrm{H}$ are obtained at a few representative laboratory energies between 10 and 400 eV by normalization to the known detachment cross sections for $\mathrm{Cl}^-+\mathrm{H}_2$ [42]. Alternately, $\sigma_e(E)$ for $\mathrm{Cl}^-+\mathrm{H}$ may be obtained by direct normalization to the known values of the electron-detachment cross sections for $\mathrm{O}^-+\mathrm{H}$. Within the experimental uncertainties, both methods yield the same results for $\mathrm{Cl}^-+\mathrm{H}$, and they are in reasonable agreement with the theoretical calculation.

The total cross sections for charge transfer $\sigma_{\mathrm{CT}}(E)$ are determined by normalization to the known ion production cross sections for $\mathrm{Cl}^-+\mathrm{H}_2$ [42,43] or $\mathrm{F}^-+\mathrm{H}_2$ [42] for Cl^- and F^-, respectively, and the results for $\mathrm{I}^-+\mathrm{H}_2$ are normalized via $\mathrm{Cl}^-+\mathrm{H}_2$. $\sigma_{\mathrm{CT}}(E)$ could not be determined for $\mathrm{Br}^-+\mathrm{H}$ due to an extremely low signal-to-noise ratio for these reactants.

The measurements obtained with the present experimental apparatus are repeatable to within about 18%, and our determination of the dissociation fraction is reproducible to within 5%; additional uncertainties in the experiment amount to less than ±10% for electron-production measurements. Thus the relative uncertainty associated with the measured electron-detachment cross sections for F^-, Cl^-, Br^-, and $\mathrm{I}^-+\mathrm{H}$, reported here, is determined to be ±21%. Due to low signal-to-noise ratios, the charge-transfer cross sections determined by normalizing to the known cross sections for Cl^- or $\mathrm{F}^-+\mathrm{H}_2$ contain an uncertainty of about ±40%.

III. THEORETICAL STUDY: $\mathrm{Cl}^-+\mathrm{H}$

The traditional view of the detachment process in collisions of A^- with B invokes the formation of an unstable AB^- ion during the collision time. This ion subsequently decays by electron emission, thus leading to the detachment process. Experiments with hydrogen halide systems revealed features which could not be accounted for by a standard local complex potential approximation in which the decay of the intermediate negative ion is described via a local rate $\Gamma(R)$, which depends only on the internuclear distance R. Various approaches were then developed and tested on the hydrogen halide systems (see, e.g., [31,45]). These theoretical models included nonlocal effects in the resonance approach or used a nonresonant approach. Among the latter, the effective range approximation [17,33]—an extension of the zero-range-potential approximation [46]—was shown to be a very successful in describing collisional detachment [47,48] as well as associative detachment [18,49] and electron-molecule collisions [33]. In the effective range approach, the electron-molecule interaction is represented by a local potential $V_{\mathrm{ext}}(r)$ at large electron-molecule distances, say $r>r_0$, and the short-range interactions are described by a boundary condition at $r=r_0$ independent of the electron energy:

$$\left.\frac{1}{\psi}\frac{d\psi}{dr}\right|_{r=r_0}=f(R)\ .$$

The ZRP approach corresponds to the limit of vanishing r_0 and V_{ext}. This representation can be used in the treatment of the collision problem without any further approximation and the heavy-particle motion can be treated either quantally [18] or classically [47,48]. It is worth noting that in this approach, no resonant state is present. The HCl^- system, illustrated in Fig. 1, presents a bound state at large internuclear distances which disappears below a certain distance R_c where the ion potential-energy curve merges with that of the neutral.

The cross section for associative detachment in $\mathrm{Cl}^-+\mathrm{H}$ collisions has been previously calculated for low energies (<0.6 eV) [18] in the ZRP approximation with a quantal treatment of the nuclear motion. In the present work, we performed a study of collisional detachment at higher energies by using a semiclassical approximation which consists of determining the time evolution of the semiclassical wave packet [47,48]. The modeling for the e-HCl system, shown as the dotted line in Fig. 1, was taken from Teillet-Billy and Gauyacq [33]. This modeling was successful in reproducing the features observed for $e+\mathrm{HCl}$, viz. the vibrational excitation and the dissociative attachment cross section. Figure 2 presents the results of the present calculation for the detachment proba-

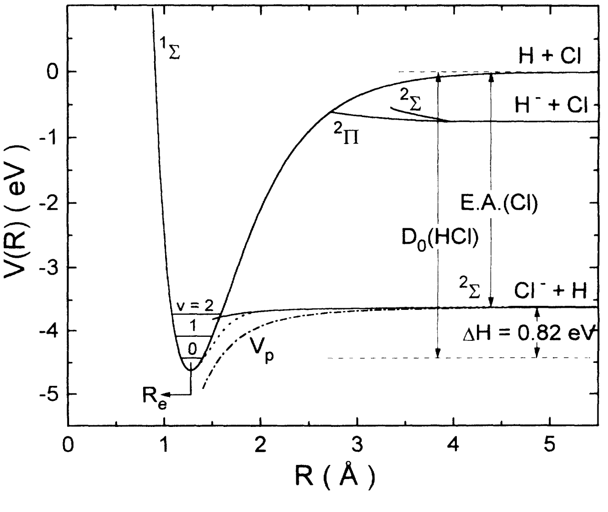

FIG. 1. Intermolecular potentials of HCl and HCl^-: HCl $^1\Sigma$ [51], solid line; HCl^- $2\,^2\Sigma$ and $^2\Pi$ [52], solid line; HCl^- $^2\Sigma$ [18], dotted line; the dipole potential V_p with $\alpha=0.7$ Å^3, dash-dotted line; the dipole potential with $\alpha'=0.14$ Å^3, solid line.

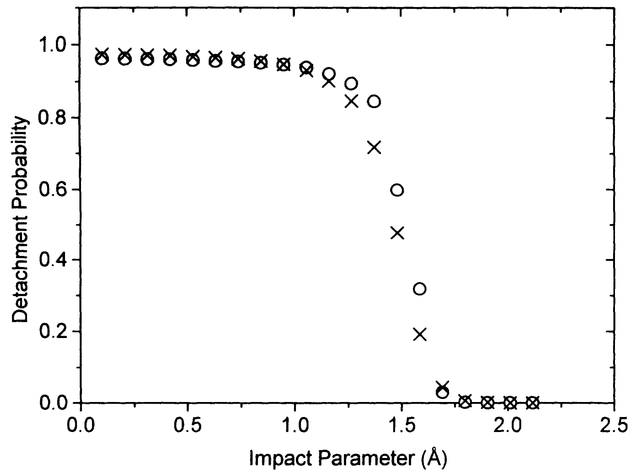

FIG. 2. Detachment probability $P_d(b)$ as a function of the impact parameter b for the system $Cl^- + H$. Open circles are the results for 4 eV and crosses correspond to 20 eV.

bility $P_d(b)$ as a function of the impact parameter b for the two collision energies 4 and 20 eV. The detachment probability exhibits a very strong dependence on b: for $b < R_c$, the system enters the unstable region and $P_d(b)$ is almost equal to one, whereas for $b > R_c$ a bound state always exists and detachment can only occur via a direct dynamic transition from the bound state to the continuum causing P_d to be very small. As a consequence, in the absence of trajectory effects, the detachment cross section is roughly equal to πR_c^2. Obviously, at low collision energies, trajectory effects appear due to the attractive ion potential and the detachment cross section increases as the energy decreases. The weak dependence of $P_d(b)$ on the collision energy can be understood by considering two opposing effects: (i) the probability for direct transitions from the bound state to the continuum increases with increasing collision velocity and (ii) the spreading of the electron wave packet in the unstable region causes the detachment probability to decrease with increasing collision velocity (see, e.g., the discussion in [50]). The net result of these dynamic effects is a very weak energy dependence of the total detachment cross section for $4 < E < 20$ eV; these results, along with the previous calculations for $E < 0.6$ eV, are shown in Fig. 3. A spline fit to these calculations is used for $\sigma_{Cl}(E_L)$ employed in Eq. (4) for the purpose of normalizing the results for F^-, Br^-, and $I^- + H$.

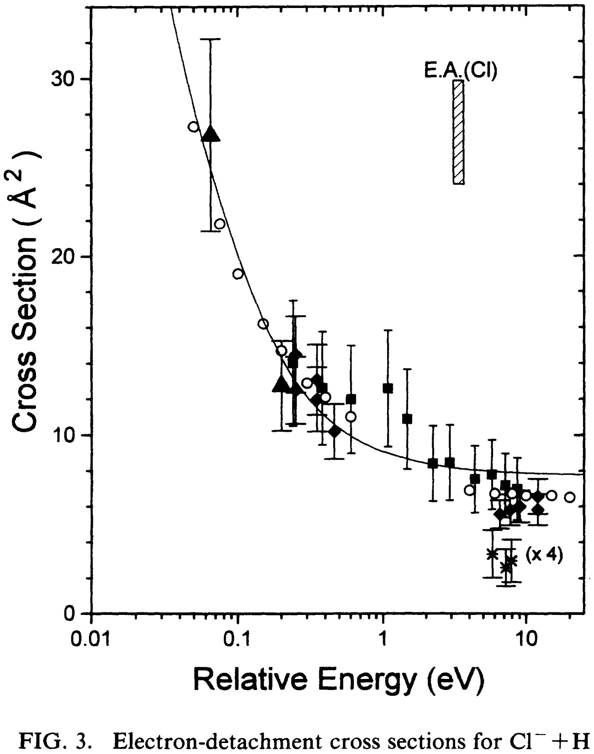

FIG. 3. Electron-detachment cross sections for $Cl^- + H$ as a function of relative collision energy. Present measurements, solid diamonds and solid squares corresponding to normalization to $Cl^- + H_2$ [42] and $O^- + H$ [3] respectively, as described in Sec. II; cross sections inferred from the reaction rates of Refs. [14,16], solid triangles; the present calculation and that of Ref. [18], open circles; and the results of the classical model described in Sec. II A with $\alpha' = 0.14$ Å^3, solid line. The asterisks represent *four times* the charge-transfer cross section.

IV. EXPERIMENTAL RESULTS AND DISCUSSION

A. $Cl^- + H$

In low-energy collisions of halogen anions with atomic hydrogen, electron loss may occur via associative detachment or collisional (direct) detachment, i.e., reactions (1) and (2). The process of AD may be discussed with the aid of Fig. 1, which illustrates the potentials of the neutral ground state of HCl ($^1\Sigma$) [51] as well as the lowest states of the transient molecular anion HCl^- representing $Cl^- + H$ ($^2\Sigma$) [18] and $H^- + Cl$ ($^2\Pi, 2\,^2\Sigma$) [52]. For relative collision energies below the EA of Cl, only AD is energetically allowed, and the system of $Cl^- + H$ evolves along the state indicated by $^2\Sigma$ in Fig. 1. This state lies above that of the neutral continuum for internuclear separations $R < R_c$, where R_c is the crossing or merging radius. The dissociation energy D_0 of HCl is larger than the EA of Cl, and this exothermicity ΔH is partitioned among the reaction products; it has been demonstrated [17,18,21,53] that almost all the exothermicity (0.82 eV) is distributed in the internal degrees of freedom of the product HCl such that the detached electron carries away less than half a vibrational quantum of energy. For relative collision energies above the EA of Cl (3.61 eV), CD may occur. Since the $^2\Sigma$ state of HCl^- is attractive into the autodetaching region, we expect no energetic threshold for AD, and, assuming near unit detachment probability for all $R < R_c$, an asymptotic (i.e., high-energy) detachment cross section $\sigma_e(E)$ of approximately πR_c^2. Various estimates of R_c for HCl^- can be found in Table I.

The experimentally determined total cross sections $\sigma_e(E)$ for electron detachment in collisions of $Cl^- + H$ for relative collision energies between 0.2 and 12 eV are shown in Fig. 3; no distinction can be made between CD and AD in the present experiment. Also shown in Fig. 3 are cross sections derived from previous rate constant measurements [14,16]; these are in good agreement with the present results. The open circles represent the previously discussed ZRP calculations for relative collision energies below 0.6 eV [18] and the present work for $4 < E < 20$ eV. It is immediately evident from Fig. 3 that the calculated cross sections show good agreement with the measurements over the entire energy range investigated and, within the limits of the experimental uncertainties, correctly predict a detachment cross section of about 6.5 Å^2 at the highest collision energy.

In a simple model [40], which has been used to describe associative and collisional detachment, the anion-atom interaction is approximated by a point charge induced dipole potential given by

$$V_p(R) = -\frac{\alpha e^2}{8\pi\epsilon_0 R^4} , \tag{5}$$

where R is the internuclear separation and α is the polarizability of the target. In this simple model, detachment is assumed to occur when the impact parameter is such that classical orbiting takes place. Such orbiting occurs for a potential of the form given by (5) when $b < b_L$, where

$$b_L = (\alpha e^2 / 2\pi\epsilon_0 E)^{1/4} . \tag{6}$$

The resulting (Langevin) orbiting cross section in then πb_L^2 or

$$\sigma_L = \frac{k_L}{v} = \frac{e}{v}\left[\frac{\pi\alpha}{\mu\epsilon_0}\right]^{1/2} , \tag{7}$$

where v and μ are the collision velocity and reduced mass of the system and k_L is the Langevin reaction rate $k_L = e(\pi\alpha/\mu\epsilon_0)^{1/2}$. For atomic hydrogen α has a value of 0.7 Å^3 and thus k_L is predicted to be about 2×10^{-9} cm^3/sec.

For higher collision energies this orbiting model will underestimate the cross section as it fails to account for curve crossing which can occur for $b > b_L$. In particular for $E > E_0 = \alpha e^2/8\pi\epsilon_0 R_c^4 = -V_p(R_c)$ [40], the orbiting detachment cross section is no longer given by (7) but by

$$\sigma_e(E) = \pi R_c^2 \left[1 + \frac{E_0}{E}\right] . \tag{8}$$

Thus E_0 defines the "transition" energy from an orbiting to a curve-crossing dominated region.

If the polarizability of hydrogen (0.7 Å^3) is used in Eq. (5) for $V_p(R)$, the resulting potential (denoted V_p in Fig. 1) falls well below any reasonable estimate of the true interaction potential. Clearly if one is to take advantage of the analytic simplicity of the orbiting model, the static polarizability of hydrogen (0.7 Å^3) must be replaced by a smaller "effective" polarizability α' in order for (5) to mimic the molecular anion potential. In light of the above discussion, we take the following approach in order to provide a simple model which describes the detachment process: We assume an interaction potential of the form given by (5), except we replace α by an effective polarizability α', which is determined by R_c from the calculations of Goldstein, Segal, and Wetmore [54] (see Table I) and $V(R_c)$ from the Morse potential for the neutral molecule [51]. In Fig. 1 we show the resulting potential for $\alpha' = 0.14$ Å^3 ($R_c = 1.57$ Å, $E_0 = 0.17$ eV) and, as mentioned previously, the induced dipole potential with $\alpha = 0.7$ Å^3. This particular value for R_c and hence α' is chosen because the resulting detachment cross sections determined by (7) and (8), shown in Fig. 3, best matches the present data as well as previous rate constant measurements.

It should be mentioned that certain problems arise in determining $V(R_c)$ and hence α' from the calculations listed in Table I. Many of the anion potential curves from Table I are presented in the literature as difference potentials and are not accurate when referenced to a Morse potential (for the neutral species) which has been inferred from spectroscopic data. In most cases, this problem occurs because the calculated neutral potential curves (of the same species) differ considerably from the Morse potential. Specifically, if the energy difference between the calculated anion potential and neutral parent is subtracted from the Morse potential, then the resulting anion potentials display barriers not present in the original representation. If, on the other hand, the calculated anion curve is directly compared to the Morse potential for the neutral molecule then the crossings may not occur at the same point. In summary, the principal useful feature of almost all of the calculations listed in Table I is the merging, or crossing, distances for the anion-neutral systems. This merging radius R_c and the known potential for the neutral molecule can be used to find α'. We will employ this procedure to model the interactions for F^- and $Br^- + H$ in the discussions that follow.

Finally a few words about charge transfer for collisions of $Cl^- + H$. Charge exchange leading to $H^- + Cl$ is endothermic by 2.85 eV and hence cannot occur for laboratory energies below 100 eV. From Fig. 1 it may be seen that the two lowest states of $H^- + Cl$ are repulsive outside the autodetaching region and do not approach the $^2\Sigma$ state of $Cl^- + H$. Since the lifetime of HCl^- inside the autodetaching region is very short, charge transfer would have to occur before either of the curves cross into the HCl continuum. The charge-transfer probability is roughly proportional to $\exp[-\Delta E(R) b/\hbar v]$, where v is the collision velocity and $\Delta E(R)$ represents the energy difference between, e.g., the $^2\Sigma$ state of $Cl^- + H$ and the $^2\Pi$ state of $H^- + Cl$. From Fig. 1, $\Delta E(R) \geq 2.85$ eV for all R; thus the charge-transfer probability is expected to be very small for the range of laboratory energies sampled in this study. The notion that the $^2\Pi$ and $2\,^2\Sigma$ states of $H^- + Cl$ are repulsive is supported by the observation that in electron-scattering experiments on HCl, the H^- production cross section suggests the presence of two dissociative anion resonances of HCl^-, located at about 7 and 9 eV in the Franck-Condon region of the HCl($v = 0$) molecule [55]; this implies that the two lowest states of $H^- + Cl$ are repulsive. In the present measurements, the charge-transfer cross section is indeed found to be small; the results are presented in Fig. 3.

In conclusion it may be stated that the electron-detachment cross section for $Cl^- + H$ is fairly well characterized for laboratory energies below 500 eV. We will take advantage of this by using $Cl^- + H$ to normalize the results for the other reactants. In particular, the calculation of $\sigma_e(E)$ discussed in Sec. III will be used for the simple normalization procedure described by Eq. (4).

B. F^- and $Br^- + H$

The total electron-detachment cross sections for $F^- + H$ are presented in Fig. 4 as a function of relative collision energy. For collision energies below 3.4 eV, i.e., the electron affinity of F, only associative detachment is energetically allowed. Also shown in the figure is the associative detachment cross section inferred from the thermal reaction rate measurement of Fehsenfeld [14], specifically $k_{AD} = 1.6 \times 10^{-9}$ cm^3/sec at 300 K (or about 0.04 eV), which is about $0.82 k_L$. This is comparable to $k_{AD} = 1.5 \times 10^{-9}$ cm^3/sec, reported by Smith and Adams [15] for the same reactants at 300 K. These latter authors, however, report that the AD reaction rate is diminished by a factor of 2 at 500 K (or 0.067 eV).

Also shown in Fig. 4 are the results of the classical model discussed above. In this case, we use $R_c = 1.06$ Å from Segal and Wolf [22] with $\alpha' = 0.4$ Å^3 and $E_0 = 2.26$ eV. The model predicts a cross section which is in agreement with our results and the rate measurements at 300 K. The modified polarization potential with $\alpha' = 0.4$ Å^3 presented in Fig. 5(a) clearly provides an excellent approximation to the $^2\Sigma$ potential for HF^- taken from Segal and Wolf. The rate measurement at 500 K does not seem to be compatible with the present results; the reason for this apparent discrepancy is not understood. The small charge-transfer cross section for $F^- + H$ is also shown in Fig. 4.

Total electron-detachment cross sections for $Br^- + H$ are shown in Fig. 6, as well as cross sections determined from previous reaction rate measurements [15]; the present results are in good agreement with the reaction rates. The cross section which results from the classical model with $R_c = 1.65$ Å, $\alpha' = 0.09$ Å^3, and $E_0 = 0.09$ eV is also shown in Fig. 6. The particular value for R_c was chosen such that the resulting cross sections best matched the present measurements. This value (1.65 Å)

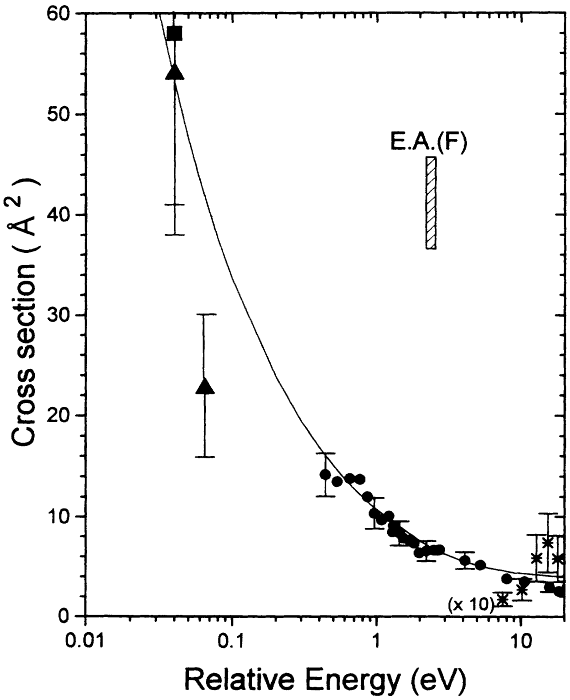

FIG. 4. Electron-detachment cross sections for $F^- + H$ as a function of relative collision energy. Present measurement, solid circles; cross sections inferred from the reaction rates of Ref. [14], solid square; and of Ref. [15], solid triangles; and the results of the classical model described in Sec. IV A with $\alpha' = 0.4$ Å^3, solid line. The asterisks represent *ten times* the charge-transfer cross section.

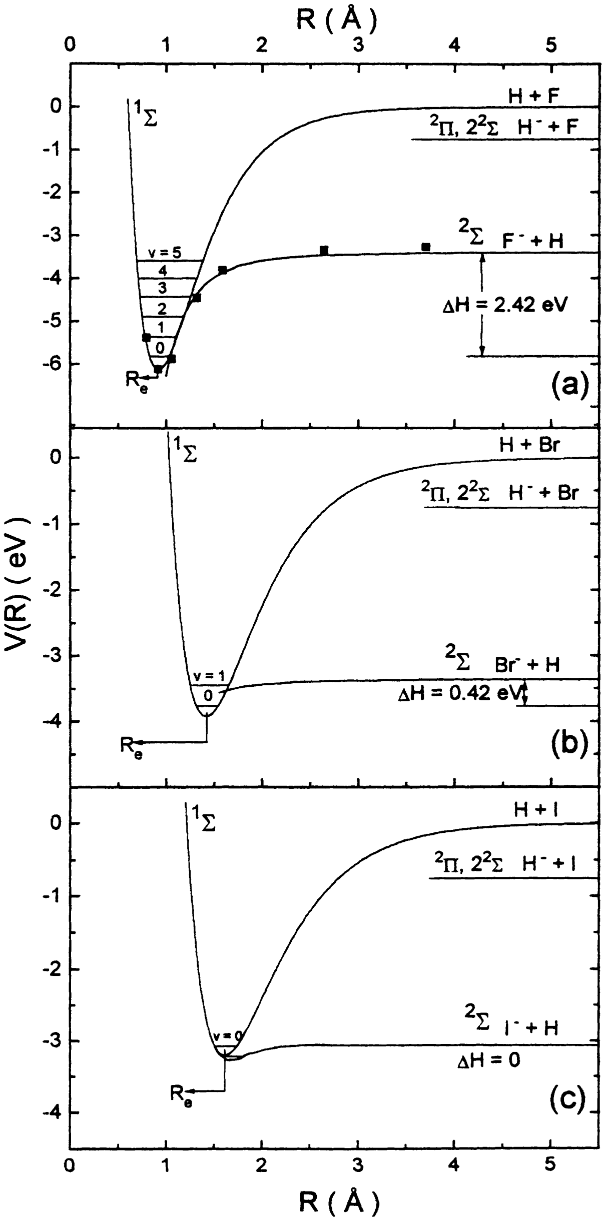

FIG. 5. Intermolecular potentials for (a) HF $^1\Sigma$ [51], solid line; HF^- $^2\Sigma$ [22], solid squares; dipole potential with $\alpha' = 0.4$ Å^3, solid line; (b) HBr $^1\Sigma$ [51], solid line; polarization potential with $\alpha' = 0.09$ Å^3, solid line; (c) HI $^1\Sigma$ [51], solid line; HI^- $^2\Sigma$ schematic inferred from present results, solid line.

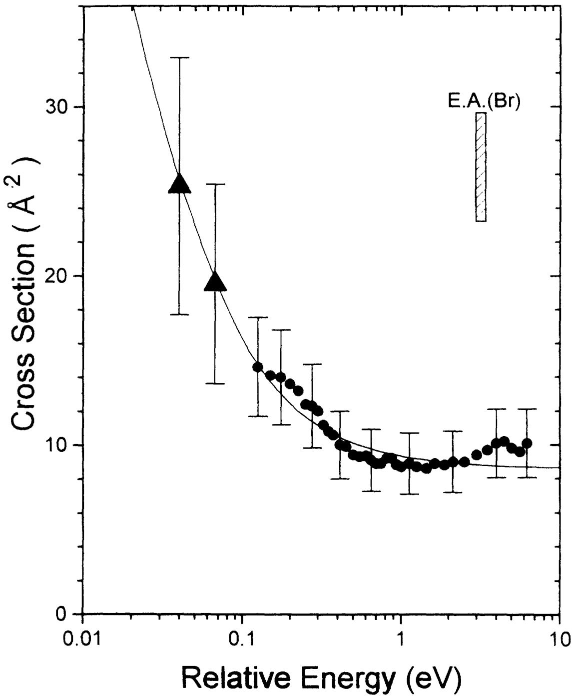

FIG. 6. Electron-detachment cross sections of $Br^- + H$ as a function of relative collision energy. Present measurements, solid circles; cross sections inferred from the reaction rates of Ref. [15], solid triangles; results of the classical model described in Sec. IV A with $\alpha' = 0.09$ Å^3, solid line.

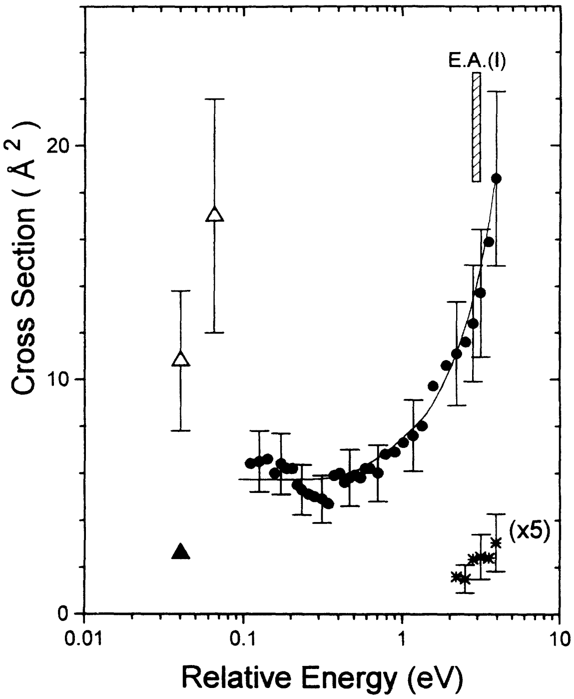

FIG. 7. Cross sections for electron detachment and charge transfer for $I^- + H$. Present results for detachments, solid circles; *five times* the present results for charge transfer, asterisks; detachment cross sections inferred from the reaction rates of Ref. [15], open triangles; and of Ref. [14], solid triangle. The solid line is a guide to the eye.

is slightly smaller than the merging radius $R_c = 1.72$ A calculated by Chapman, Balasubramanian, and Lin [39]. It should be noted that V (1.72 Å), where $V(R)$ is the Morse potential for HBr, lies slightly *above* the asymptotic limit for $Br^- + H$, implying a barrier to AD. Figure 5(b) depicts the Morse potential for HBr [51] and the polarization potential with $\alpha' = 0.09$ Å^3. We were unable to determine a statistically significant charge-transfer cross section for $Br^- + H$.

The similarity of $\sigma_e(E)$ for $Br^- + H$ at low energies to that for $Cl^- + H$ indicates that analogous detachment mechanisms are involved and that the non-Born-Oppenheimer effects, indicated in the ZRP model, play similar roles in both cases. Indeed the two systems are comparable in many respects; both have an exothermicity (for AD) which is small, 0.42 eV for $Br^- + H$ and 0.82 eV for $Cl^- + H$, compared to the large ΔH of about 2.42 eV for $F^- + H$. The number of accessible vibrational states for the AD products is two for HCl and one for HBr, compared to five for the HF products. This, and the apparent similarity of the HF^- $^2\Sigma$ state to the induced polarization potential with $\alpha' = 0.4$ Å^3, may explain why electron detachment in collisions of F^- with H is adequately described by a simple orbiting model over the entire energy range investigated.

C. $I^- + H$

Presented in Fig. 7 are the detachment cross sections for $I^- + H$ as a function of relative collision energy. The EA of iodine is 3.059 eV [1] and the dissociation energy of HI ($^1\Sigma$) is 3.054 eV [51]. Thus associative detachment for $I^- + H$ is slightly endothermic. In this respect $I^- + H$ is different from the previous halogen hydride systems investigated here. From Fig. 7 it is evident that the $\sigma_e(E)$ for $I^- + H$ displays a dramatically different behavior when compared to F^-, Cl^-, or $Br^- + H$. The detachment cross section for $I^- + H$ is relatively constant between 0.09 and 1.2 eV and then increases sharply with energy above the threshold for which direct detachment is energetically possible. The rate constants for associative detachment have been measured [15] by Smith and Adams at about 300 and 500 K, and the cross sections inferred from their measurements are also indicated in Fig. 7. These results appear to be incompatible with the present measurements and that inferred from a 300-K rate measurement by Fehsenfeld [14].

The charge-transfer cross section $\sigma_{CT}(E)$ for $I^- + H$ is observed to increase slowly with energy from about 0.3 to 0.6 Å^2 for relative collision energies between 2.2 and 4 eV. Charge transfer in $I^- + H$ is endothermic by about 2.3 eV; although an energetic threshold for $\sigma_{CT}(E)$ is not directly apparent, the cross section extrapolates to an experimental threshold of approximately 1.5 eV. The difference of 0.8 eV from the energetically allowed threshold may be accounted for by thermal broadening [56].

An additional aspect of HI, which sets it apart from the previously discussed halogen hydrides, is that it forms a stable negative ion [57,58]. Thus the $HI^-(^2\Sigma)$ potential must support at least the lowest vibrational state, which requires a well depth of about 0.15–0.2 eV based on the vibrational ground state of HI. A few conclusions about the $^2\Sigma$ state may be drawn from the measured detachment cross sections. At the lowest collision energies, $\sigma_e(E)$ is constant at about 6.3 ± 1.1 Å^2, and no evidence for a rapid decrease with decreasing collision energy is observed. If indeed an energetic threshold exists for associative detachment, then, based on the present measurements, it is expected to be less than or equal to about 0.1 eV. This observation is compatible with the calculations of Chapman, Balasubramanian, and Lin [39], who report an energetic threshold of 0.1 eV for AD, and also with the experimental results of Alajajian and Chutjian [38], who suggest a threshold of less than 0.1 eV, based upon their dissociative attachment measurements. Rydberg electrons in laser-pumped alkali-metal atoms have been used by Carman, Klots, and Compton [58] to investigate dissociative and nondissociative capture in HI and the low-energy cross sections inferred from their study (and the lack of and discernable energetic threshold) are compatible with the observations of Alajajian and Chutjian [38]. This low-energy behavior is also in agreement with the rate measurements of Fehsenfeld [14] if thermal broadening is considered.

The question of just where the HI^- potential merges with that of HI has been discussed in some detail by Carman, Klots, and Compton [58]. If one assumes that the detachment cross section is given simply by πR_c^2, then our present results would indicate that R_c is slightly less than the HI equilibrium separation of 1.6 Å. The results of dissociative attachment experiments by Alajajian and Chutjian led them to suggest a crossing radius which is approximately equal to the equilibrium separation of HI, whereas the calculations of Chapman, Balasubramanian, and Lin give $R_c=1.9$ Å. Carman, Klots, and Compton argue that this calculated value (1.9 Å) is too large and that the merging of the two potentials should occur for $R \gtrsim R_e$. The present results tend to support the argument that R_c is substantially less than 1.9 Å if indeed the near-threshold cross section is given by πR_c^2. An intermolecular potential for HI^- with $R_c \simeq 1.6$ Å and a well depth of about 0.2 eV is presented in Fig. 5(c).

Finally, the disagreement of the detachment cross sections at the lowest energies reported here with previous rate constant measurements of Smith and Adams is not understood. Their experimental method used to obtain the thermal reaction rates for AD in $\mathrm{I}^-+\mathrm{H}$ (and Br^- and $\mathrm{F}^-+\mathrm{H}$) is self-consistent, and no systematic error is evident in their measurements which might be specific to $\mathrm{I}^-+\mathrm{H}$ that would explain the discrepancy with the measured cross sections reported here or the rate constant measurements of Fehsenfeld [14]. It should be noted that if their result, obtained at 300 K, is normalized to the measurement of Fehsenfeld, then their high-energy data point agrees reasonably well with the lowest-energy measurement presented here.

V. SUMMARY AND CONCLUSION

The electron-detachment cross sections $\sigma_e(E)$ for collisions of $\mathrm{Cl}^-+\mathrm{H}$ have been measured for relative collision energies below 20 eV, and are in good agreement with previous rate constant measurements and a ZRP-type calculation. The detachment cross section for $\mathrm{Cl}^-+\mathrm{H}$ has also been described by a classical orbiting model with a target polarizability modified to represent the principal feature of the anion-neutral interaction, viz. the distance at which the potentials for each are approximately equal. Subsequently, the system of $\mathrm{Cl}^-+\mathrm{H}$ has been used as a model system to normalize the experimental results for other reactants.

The total electron-detachment cross sections, for collisions of F^-, Br^-, and I^- with H have also been measured. The experimental results of $\sigma_e(E)$ for F^- and $\mathrm{Br}^-+\mathrm{H}$ are well described by the simple model mentioned above. For F^-, Cl^-, and $\mathrm{Br}^-+\mathrm{H}$, the measured detachment cross sections at the lowest collision energies are in good agreement with thermal rate constant measurements, and no barriers to AD are observed. This implies that the $^2\Sigma$ states of HF^-, HCl^-, and HBr^- are attractive into the autodetaching region. The modified polarizabilities which can be used to model the anion potential and hence the detachment cross section are all smaller than the known static polarizability of H. It must be emphasized that the form of the potential given by (5), along with the effective polarizability, is used only because of its analytic simplicity in the orbiting model presented in Sec. IV A. The analytic form given by (5) is thus used to approximate the intermolecular potential near R_c, and the value of R_c used to calculate α' is chosen such that the resulting detachment cross section fits the present measurements. This form does not mimic other important features of the intermolecular potential and results from a semi-empirical fit to the experimental observations.

The system of $\mathrm{I}^-+\mathrm{H}$ is found to display a quite different detachment cross section compared to those of the above halogen hydrides. The detachment cross section for $\mathrm{I}^-+\mathrm{H}$ is relatively constant for collision energies below about 1 eV. Above 1 eV, $\sigma_e(E)$ increases with increasing energy. These observations and the existence of stable HI^- underscore the difference of the $\mathrm{I}^-+\mathrm{H}$ collision system from the previously discussed halogen hydrides. Indeed, the low-energy detachment cross sections suggest a crossing radius of the HI^- $^2\Sigma$ state with the $^1\Sigma$ HI continuum which is approximately equal to the equilibrium radius R_e of the neutral HI molecule. This is in contrast to the other halogen hydride systems studied, all of which have $R_c > R_e$.

ACKNOWLEDGMENT

This work was supported in part by the U.S. Department of Energy, Office of Basic Energy Sciences, Division of Chemical Sciences.

[1] H. Hotop and W. C. Lineberger, J. Phys. Chem. Ref. Data **14**, 731 (1985); D. Hanstorp and M. Gustafsson, J. Phys. B **25**, 1773 (1992).

[2] M. A. Huels, R. L. Champion, L. D. Doverspike, and Yicheng Wang, Phys. Rev. A **41**, 4809 (1990).

[3] J. A. Fedchak, M. A. Huels, L. D. Doverspike, and R. L. Champion, Phys. Rev. A **47**, 3796 (1993).

[4] H. F. Calcote and D. E. Jensen, in *Ion-Molecule Reactions in the Gas Phase,* 152nd Meeting of the American Chemical Society, New York, edited by Piere J. Ausloos (American Chemical Society, Washington, DC, 1966), Vol. 58, p. 291ff.

[5] A. N. Haghurst and T. M. Sayden, Proc. R. Soc. London Ser. A **293**, 36 (1966).

[6] E. M. Bulewicz and P. J. Padley, Trans. Faraday Soc. **65**, 186 (1969).

[7] P. J. Chantry, in *Applied Atomic Collision Physics,* edited by E. W. McDaniel and W. L. Nighan (Academic, New York, 1982), Vol. 3, p. 35ff.

[8] M. Rokui and J. H. Jacob, in *Applied Atomic Collision Physics* (Ref. [7]), p. 273ff.

[9] W. L. Nighan, in *Applied Atomic Collision Physics* (Ref. [7]), p. 319ff.

[10] H. S. W. Massey, in *Applied Atomic Collision Physics,* edited by H. S. W. Massey and D. R. Bates (Academic, New Yorok, 1982), Vol. 1, pp. 7ff and 105ff.

[11] H. I. Schiff, in *Applied Atomic Collision Physics* (Ref. [10]) p. 293ff.

[12] H. S. W. Massey, in *Applied Atomic Collision Physics* (Ref. [10]), p. 235ff.

[13] E. E. Ferguson, in *Kinetics of Ion-Molecule Reactions,* edited by Piere J. Ausloos (Plenum, New York, 1978), p. 377.

[14] F. C. Fehsenfeld, in *Interactions between Ions and Molecules,* edited by Piere J. Ausloos (Plenum, New York, 1975), p. 387ff.

[15] D. Smith and N. G. Adama, J. Phys. B **20**, 4903 (1987).

[16] C. J. Howard, F. C. Fehsenfeld, and M. McFarland, J. Chem. Phys. **60**, 5086 (1974).

[17] J. P. Gauyacq, *Dyanmics of Negative Ions* (World Scientific, Singapore, 1987).

[18] J. P. Gauyacq, J. Phys. B **15**, 2721 (1982).

[19] S. E. Haywood and J. B. Delos, Chem. Phys. **145**, 253 (1990).

[20] T. S. Zwier, J. C. Weisshaar, and S. R. Leone, J. Chem. Phys. **75**, 4885 (1981).

[21] T. S. Zwier, M. Matti Maricq, C. J. S. M. Simpson, Veronica M. Bierbaum, G. Barney Ellison, and S. R. Leone, Phys. Rev. Lett. **44**, 1051 (1980).

[22] G. A. Segal and K. Wolf, J. Phys. B **14**, 2291 (1981).

[23] M. Bettendorff, R. J. Buenker, and S. D. Peyerimhoff, Mol. Phys. **50**, 1363 (1983).

[24] L. A. Morgan and P. G. Burke, J. Phys. B **21**, 2091 (1988).

[25] T. Gorczyca and D. W. Norcross, Phys. Rev. A **45**, 140 (1992).

[26] L. A. Morgan, P. G. Burke, and C. J. Gillian, J. Phys. B **23**, 99 (1990).

[27] K. Rohr and F. Linder, J. Phys. B **9**, 2521 (1976).

[28] R. Abouaf and D. Teillet-Billy, J. Phys. B **10**, 2261 (1977).

[29] R. Allan and S. F. Wong, J. Chem. Phys. **74**, 1687 (1981).

[30] L. Dube and A. Herzenberg, Phys. Rev. Lett. **38**, 820 (1977).

[31] *Aspects of Electron-Molecule Scattering and Photoionization,* edited by A. Herzenberg, AIP Conf. Proc. No. 204 (AIP, New York, 1989).

[32] J. G. Gauyacq and A. Herzenberg, Phys. Rev. A **25**, 2959 (1982).

[33] D. Teillet-Billy and J. P. Gauyacq, J. Phys. B **17**, 4041 (1984).

[34] W. Domcke and C. Mundel, J. Phys. B **18**, 4491 (1985).

[35] I. I. Fabrikant, S. A. Kalin, and A. K. Kazansky, J. Chem. Phys. **95**, 6566 (1991); J. Phys. B **25**, 2885 (1992).

[36] G. Knoth, M. Rädle, H. Ehrhardt, and K. Jung, Europhys, Lett. **4**, 805 (1987); G. Knoth, M. Rädle, M. Gote, H. Ehrhardt, and K. Jung, J. Phys. B **22**, 299 (1989); M. Rädle, G. Knoth, K. Jung, and H. Ehrhardt, *ibid.* **22**, 1455 (1989).

[37] M. A. Morrison, Adv. At. Mol. Phys. **24**, 51 (1988).

[38] S. H. Alajajian and A. Chutjian, Phys. Rev. A **37**, 3680 (1988).

[39] D. A. Chapman, K. Balasubramanian, and S. H. Lin, Phys. Rev. A **38**, 6098 (1988).

[40] A. Herzenberg, Phys. Rev. **160**, 80 (1967).

[41] J. Slevin and W. Sterling, Rev. Sci. Instrum. **52**, 1780 (1981).

[42] M. S. Huq, D. S. Fraedrich, L. D. Doverspike, R. L. Champion, and V. A. Esaulov, J. Chem. Phys. **76**, 4952 (1982).

[43] L. D. Doverspike, B. T. Smith, and R. L. Champion, Phys. Rev. A **22**, 393 (1980).

[44] M. S. Huq, L. D. Doverspike, and R. L. Champion, Phys. Rev. A. **27**, 785 (1983).

[45] J. P. Gauyacq and D. Teillet-Billy, in *Negative Ions,* edited by V. Esaulov (Cambridge University Press, Cambridge, England, 1994).

[46] Yu. N. Demkov, Zh. Eksp. Teor. Fiz. **46**, 1126 (1964), [Sov. Phys.—JETP **19**, 762 (1964)].

[47] J. P. Gauyacq, J. Phys. B **13**, 4417 (1980).

[48] J. P. Gauyacq, Y. Wang, R. C. Champion, and L. D. Doverspike, Phys. Rev A **38**, 2284 (1988).

[49] J. P. Gauyacq, J. Phys. B **16**, 4049 (1983).

[50] J. P. Gauyacq, Comments At. Mol. Phys. **10**, 171 (1981).

[51] K. P. Huber and G. Herzberg, *Molecular Spectra and Molecular Structure IV, Constants of Diatomic Molecules* (Van Nostrand and Reinhold, New York, 1979).

[52] S. V. O'Neil, P. Rosmus, and D. W. Norcross, J. Chem. Phys. **85**, 7232 (1986).

[53] M. A. Smith and S. R. Leone, J. Chem. Phys. **78**, 1325 (1983).

[54] E. Goldstein, G. A. Segal, and R. W. Wetmore, J. Chem. Phys. **68**, 271 (1978).

[55] R. Azria, L. Roussier, R. Paineau, and M. Tronc, Rev. Phys. **9**, 469 (1974).

[56] P. J. Chantry, J. Chem. Phys. **55**, 2746 (1971).

[57] D. Spence, W. A. Chupka, and C. M. Stevens, J. Chem. Phys. **76**, 2759 (1982).

[58] H. S. Carman, Jr., C. E. Klots, and R. N. Compton, J. Chem. Phys. **99**, 1734 (1993).

[59] P.-O. Åstrand and G. Karlström, Chem. Phys. Lett. **28**, 624 (1990).

[60] M. Krauss and W. J. Stevens, J. Chem. Phys. **74**, 570 (1981).